

# $\alpha$ cluster structures in unbound states of $^{19}\text{Ne}$

R. OTANI, M. IWASAKI and M. ITO

Department of Pure and Applied Physics, Kansai University, 3-3-35  
Yamatecho, Suita, Osaka 564-8680, Japan

## Abstract

Cluster structures in  $^{19}\text{Ne}$  are studied by the microscopic and macroscopic cluster models. In the microscopic calculation, the coupled-channels problem of  $(\alpha+^{15}\text{O}) + (^3\text{He}+^{16}\text{O})$  are solved, and the calculated energy spectra nicely reproduce the low-lying levels. In the macroscopic approach, the  $\alpha + ^{15}\text{O}$  potential model is applied. The calculation of the potential model predicts the existence of the resonances above the  $\alpha$  threshold, which has a weak-coupling structure of the  $\alpha$  particle plus one hole inside of the  $^{16}\text{O}$  nucleus. The coupling effect of the  $5p-2h$  configuration to  $^{19}\text{Ne}$  is briefly discussed.

## 1 Introduction

The  $\alpha$  cluster structures have been extensively studied for the so-called  $4N$  nuclei with  $N = Z$ , such as  $^8\text{Be} = 2\alpha$ ,  $^{12}\text{C} = 3\alpha$ ,  $^{16}\text{O} = \alpha + ^{12}\text{C}$ , and  $^{20}\text{Ne} = \alpha + ^{16}\text{O}$  [1]. In current studies, the importance of the cluster degrees of freedom has been extended to the neutron-rich ( $N > Z$ ) systems, which are obtained by adding extra neutrons to the  $4N$  cluster systems. In the neutron-rich systems, various chemical-bonding-like structures are generated by the coupling of the cluster relative motion and the single particle motion of extra neutrons [2–4].

On the contrary, cluster structures in the  $4N$  systems with a hole in a cluster core, are also interesting research subjects [5, 6]. Pioneering work of the hole system is the study of the  $^{19}\text{F}$  nucleus [5, 6]. In the  $\alpha + ^{15}\text{N}$

system, a proton hole inside of the  $^{16}\text{O}$  core weakly couples to the relative motion of the binary cluster cores. The weak coupling state of the hole in  $^{16}\text{O}$  and the  $\alpha$  particle is also expected in the neutron-deficient system,  $\alpha + ^{15}\text{O}$  in  $^{19}\text{Ne}$  [5, 6]. However, detailed analysis of the energy levels over a wide energy region, which covers the unbound continuum states, have not been undertaken.

Recently, we have applied the potential model to the  $\alpha + ^{15}\text{O}$  system [7] and predicted the existence of the resonances above the  $\alpha$  threshold and the excitation function of the  $\alpha$  resonant scattering. The potential model is useful to understand the resonant states, in which the  $\alpha$  clustering is well developed. However, the microscopic cluster model on the basis of the nucleon degrees of freedom is very important in analyzing the energy levels from the low-lying states to the highly-excited states in a unified manner. In the present report, we apply the microscopic cluster model of  $(^3\text{He} + ^{15}\text{O}) + (\alpha + ^{16}\text{O})$  and mainly analyze the low-lying states in  $^{19}\text{Ne}$ .

There is another reason why we focus on the  $\alpha + ^{15}\text{O}$  structure in the  $^{19}\text{Ne}$  nucleus. The  $^{15}\text{O}(\alpha, \gamma)^{19}\text{Ne}$  reaction is known to play a crucial role in the advanced stages of astrophysical hydrogen burning [8]. The most crucial resonance is known to arise through the  $3/2^+$  resonance level at 504 keV with respect to the  $\alpha + ^{15}\text{O}$  threshold ( $E_x = 4.03$  MeV). The analyses in Ref. [9] have pointed out that the intrinsic structure of the resonance at 504 keV in  $^{19}\text{Ne}$  is the five particle–two hole ( $5p-2h$ ) configuration with the  $^{14}\text{O}_{g.s.}$  core. The  $5p-2h$  configuration has a large overlap with the shell model limit of the  $^5\text{He} + ^{14}\text{O}$  configuration. Thus, the coupling effect of  $^5\text{He} + ^{14}\text{O}$  on the  $J^\pi = 3/2^+$  is also discussed.

## 2 Framework

We apply the generalized two-center cluster model (GTCM) for the calculations of the low-lying levels. The GTCM is the extended model of the microscopic cluster model on the basis of the generator coordinate method (GCM) [10]. The application of GTCM to Be isotopes has already been published in Ref. [2], and we briefly explain the formulation of GTCM in the  $^{19}\text{Ne}$  nucleus. The basis function for  $^{19}\text{Ne}$  is given by

$$\Phi^{J^\pi K}(S) = \hat{P}_K^{J^\pi} \mathcal{A} \left\{ \psi(^3\text{He})\psi(^{14}\text{O}) \prod_{j=1}^2 \varphi_j(m_j) \right\}_S. \quad (1)$$

The basis function is constructed on the basis of the  $^3\text{He} + ^{14}\text{O}$  cores, and the two neutrons are treated as the active valence-nucleons. The  $\psi(^3\text{He})$

and  $\psi(^{14}\text{O})$  represent the core wave functions of the  $^3\text{He}$  and  $^{14}\text{O}$  nuclei, respectively. The former part is described by the  $(0s)^3$  configuration in the harmonic oscillator (HO) potential, while the latter part is constructed by the  $(0s)^4(0p)^{10}$  configuration. Two core nuclei are placed with the relative distance parameter  $S$ . The single-particle wave function for the  $j$ th valence neutrons ( $j = 1, 2$ ) localized around the  $^3\text{He}$  or  $^{14}\text{O}$  cluster is given by an atomic orbital (AO)  $\varphi(m_j)$ , which is classified by a set of the AO quanta  $m_j = (k, C, \tau)$  with the labels of the Brink orbitals  $k$ , the core  $C$ , and the neutron spin  $\tau$  ( $= \uparrow$  or  $\downarrow$ ). The Brink orbitals around the core  $C$  ( $C = ^3\text{He}$  or  $^{14}\text{O}$ ) are  $k = 0s$  for  $C = ^3\text{He}$  and  $k = 0p$  for  $C = ^{14}\text{O}$ . The basis functions with the full anti-symmetrization  $\mathcal{A}$  are projected to the eigenstate of the total spin  $J$ , its intrinsic angular projection  $K$ , and the total parity  $\pi$  by the projection operator  $\hat{P}_K^{J\pi}$ .

In the present calculation, we solve the coupled-channels problem of  $(^3\text{He}+^{16}\text{O}) + (\alpha+^{15}\text{O})$  at a fixed  $S$  and calculate the adiabatic energy curves, which are the sequence of the energy eigenvalues as a function of the distance parameter  $S$  [2]. We search the energy minimum in the energy curves calculated for the individual spin-parity states. The distance parameter  $S$  is the variational parameter, which is called the generator coordinate [10]. The superposition of  $S$  is possible but we fix  $S$  to the minimum point in evaluating the energy levels. As for the nucleon-nucleon (NN) interaction, we use the Volkov No.2 [11] and the G3RS [12] for the central and spin-orbit parts, respectively. The parameters in the NN interactions and the size parameter of HO are tuned to reproduce the  $^3\text{He}$  and  $^4\text{He}$  decay thresholds in  $^{19}\text{Ne}$  as much as possible.

The macroscopic potential model is also applied to calculate the unbound resonant states [7]. The Woods Saxon (WS) potential is assumed for the nuclear potential in  $\alpha + ^{15}\text{O}$ , and its parameter set is fixed so as to reproduce the angular distribution of the  $\alpha + ^{15}\text{N}$  elastic scattering. The resonant levels are calculated from the  $\alpha + ^{15}\text{N}$  potential by adding the Coulomb force. Above the  $\alpha$  decay threshold, the absorbing boundary condition (ABC) [13] is applied to identify the resonant levels. The detailed explanations of the potential model plus ABC is shown in Ref. [7].

### 3 Results

In Fig. 1, the calculated spectra (middle and right levels) are compared with the experimental data (left levels). The results of the negative parity states are shown in this figure. The middle levels is obtained by the microscopic

model of  $({}^3\text{He}+{}^{16}\text{O}) + (\alpha+{}^{15}\text{O})$ , while the right levels is the result of the potential model. The microscopic calculation reproduces the level ordering of the low-lying bound spectra in the experiment although the level spacing of the theoretical calculation is a little different from the experimental levels.

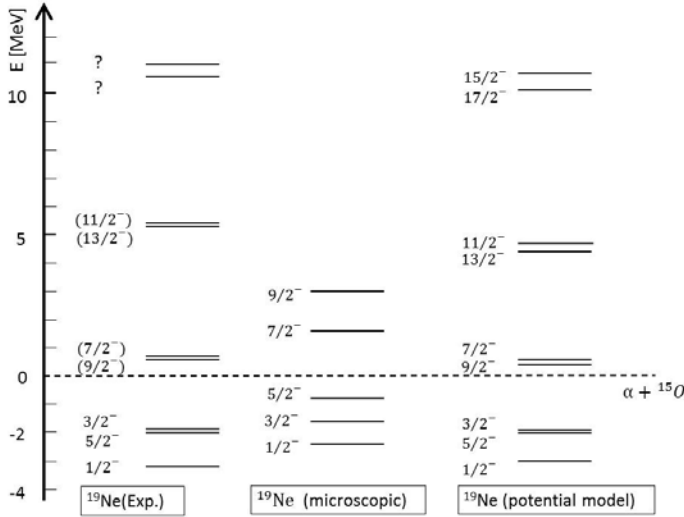


Figure 1: Energy levels of the negative parity states in the  ${}^{19}\text{Ne}$  nucleus. The left levels are the experimental data, while the middle and right levels are the results of the microscopic and macroscopic models, respectively. The dotted line represents the  $\alpha$  threshold energy, which is set to the zero energy.

In the potential model calculation, the low-lying bound levels are nicely reproduced. Furthermore, the potential model under the absorbing boundary condition predicts the resonant levels above the  $\alpha$  threshold. Unfortunately, the experimental information is still insufficient in the unbound region. Thus, the experimental investigation of the highly-excited states are strongly desired.

The result of the positive parity states are shown in Fig. 2. The microscopic calculation with  $({}^3\text{He}+{}^{16}\text{O}) + (\alpha+{}^{15}\text{O})$  is shown at the center, while the experimental levels and the result of the potential model are plotted at the left and right positions, respectively. The relative wave function of the  $\alpha+{}^{15}\text{O}$  cluster configuration in the microscopic calculation (middle levels) corresponds to the HO states with the total oscillator quantum of  $N = 7$ , while the resonant levels obtained by the potential model (right levels) belong to the one higher nodal state,  $N = 9$ . The microscopic calculation reproduces the level ordering of the experiment in the bound region. The macroscopic calculation predicts the existence of the resonant states with

the higher spins of  $J^\pi \geq 11/2^+$  and hence, the experimental investigation of these resonances is interesting.

Both the microscopic and macroscopic calculations do not reproduce the  $J^\pi = 3/2^+$  state existing around the  $\alpha$  threshold. This failure is the same as the results of the previous coupled-channel OCM calculation in  $^{19}\text{F} = ({}^3\text{H}+{}^{16}\text{O}) + (\alpha+{}^{15}\text{N})$  [5]. In order to improve the calculation for the  $3/2^+$  state, we have performed the extended microscopic calculation, which is the coupled-channels of  $({}^3\text{He}+{}^{16}\text{O}) + (\alpha+{}^{16}\text{O}) + ({}^5\text{He}+{}^{14}\text{O})$ , to include the  $5p$ - $2h$  configuration, which is the shell model limit ( $S = 0$ ) of  ${}^5\text{He} + {}^{14}\text{O}$ .

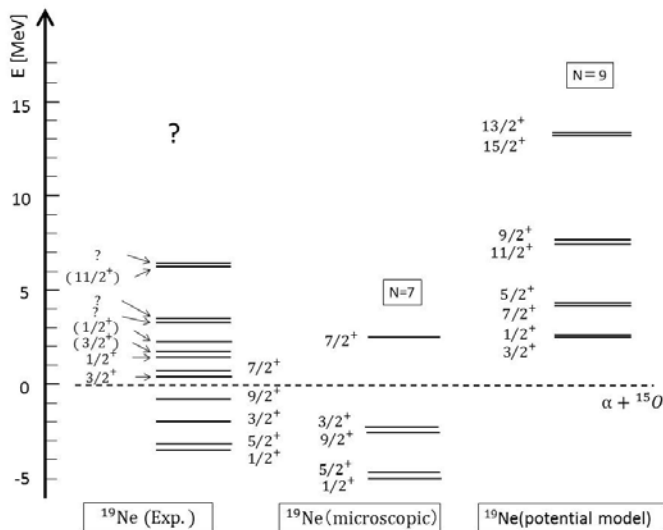


Figure 2: Same as Fig. 1 except for the positive parity states in  $^{19}\text{Ne}$ .

A new levels with a dominant component of  ${}^5\text{He} + {}^{14}\text{O}$  appear in this extended calculation. However, the energy of this  ${}^5\text{He}+{}^{14}\text{O}$  is higher by about 10 MeV than the experimental  $3/2^+$  state around the  $\alpha$  threshold. This is because the theoretical threshold energy of the  ${}^5\text{He} + {}^{14}\text{O}$  channel is also higher by about 10 MeV than the experimental threshold. Therefore, there is a possibility that a new  $3/2^+$  state appear around the  $\alpha$  threshold if the theoretical  ${}^5\text{He}$  threshold is reproduced correctly. The reproduction of the  ${}^5\text{He}$  threshold is important in the future calculation.

## 4 Summary and discussion

In sum, we have applied the microscopic and macroscopic cluster models to the level analysis of the  $^{19}\text{Ne}$  nucleus. The microscopic model is successful

in reproducing the low-lying bound spectra, while the macroscopic model predicts the existence of the several resonant states in continuum region. The experimental identification of the predicted levels is interesting in future studies.

The present calculations do not reproduce the  $3/2^+$  state, which is important in the astrophysical phenomena. The extended microscopic calculation suggests the formation of a new  $3/2^+$  state, which corresponds to the  ${}^5\text{He}+{}^{14}\text{O}$  configuration, but its excitation energy is much higher than the experimental energy. Since the failure of the  $3/2^+$  energy is due to the incorrect reproduction of the theoretical  ${}^5\text{He}$  threshold, the parameters of the NN interaction must be revised to reproduce the  ${}^5\text{He}$  threshold. The improved calculations is now underway.

## References

- [1] H. Horiuchi et al., *Suppl. Prog. Theor. Phys.* **192**, 1 (2012), and references therein.
- [2] M. Ito and K. Ikeda, *Rep. Prog. Phys.* **77**, 096301 (2014).
- [3] N. Itagaki, T. Otsuka, K. Ikeda and S. Okabe, *Phys. Rev. Lett.* **92**, 142501 (2004).
- [4] Masaaki Kimura, *Phys. Rev. C* **75**, 034312 (2007).
- [5] T. Sakuda and F. Nemoto, *Prog. Theor. Phys.* **62**, 1274 (1979).
- [6] P. Descouvemont and D. Baye, *Nucl. Phys. A* **463**, 629, (1986).
- [7] R. Otani et al., *Phys. Rev. C* **90**, 034306 (2014).
- [8] K. Langanke et al., *Astrophys. Jour.* **301**, 629 (1986).
- [9] Z. Q. Mao et al., *Phys. Rev. Lett.* **74**, 3760 (1995).
- [10] H. Horiuchi, *Suppl. Prog. Theor. Phys.* **62**, 90 (1977).
- [11] A. B. Volkov, *Nucl. Phys.* **74**, 33 (1965).
- [12] N. Yamaguchi, T. Kasahara, S. Nagata, and Y. Akaishi, *Prog. Theor. Phys.* **62**, 1018 (1979).
- [13] Y. Takenaka et al., *Prog. Exp. Theor.* **2014**, 113D04 (2014).